DALTON
FULL PAPER

Structural and photophysical properties of Ln^{III} complexes with 2,2′-bipyridine-6,6′-dicarboxylic acid: surprising formation of a H-bonded network of bimetallic entities†

Jean-Claude G. Bünzli,[a] Loïc J. Charbonnière[b] and Raymond F. Ziessel*[b]

[a] *Université de Lausanne, Institut de Chimie Minérale et Analytique, BCH-1402, CH-1015 Lausanne, Switzerland*
[b] *Laboratoire de Chimie, d'Électronique et de Photonique Moléculaire, ECPM, UPRES-A 7008 au CNRS, 25 rue Becquerel, 67087 Strasbourg Cedex 02, France*

Received 17th January 2000, Accepted 13th April 2000
Published on the Web 23rd May 2000

The ligand H_2L = 2,2′-bipyridine-6,6′-dicarboxylic acid reacts with $Ln(NO_3)_3{\cdot}xH_2O$ (x = 6, Ln = Eu, Tb; x = 5, Ln = Gd) in MeOH/Et_3N to give complexes with 1 : 2 and 2 : 3 metal : ligand stoichiometry, $(Et_3NH)[LnL_2]$ and $[Ln_2L_3(H_2O)_3]{\cdot}xH_2O$ (x = 1, Ln = Eu, Tb; x = 0, Ln = Gd) which have been isolated and characterised. A sizeable quantum yield is obtained for the 1 : 2 Eu : Ligand complex in aqueous solution (Q^{Eu}_{abs} = 11.5 ± 2.3% at pH = 6.6), pointing to an efficient ligand-to-metal energy transfer. The presence of some inner-sphere interaction with water was deduced from $Eu(^5D_0)$ lifetime measurements in water (0.86 ± 0.01 ms *vs.* 1.55 ± 0.02 ms in the solid state between 10 and 295 K, q_{est} = 0.3–0.4 water molecule). For $[TbL_2]^-$, sensitisation of Tb^{III} also occurs (Q^{Tb}_{abs} = 6.3 ± 1.3% at pH = 6.6) but the $Tb(^5D_4)$ excited level is de-populated at room temperature by a back-transfer process to the ligand. The crystal structure obtained for the 2 : 3 Tb : ligand complex evidences two distinct terbium sites, one Tb^{III} being complexed to two ligands affording a mono-anionic complex, itself linked to the second terbium ion with a μ-carboxylate bridge; the generic formulation of the crystallised complex is $[TbL_2\text{-}\mu\text{-}TbL(H_2O)_3]{\cdot}2H_2O{\cdot}$ 2MeOH. Consecutive dimers are linked by an elaborate network of H-bonds involving interstitial solvent molecules. A photophysical study of the 2 : 3 Eu : Ligand complex in the solid state points to the same structural features, revealing two metal ion sites with essentially no bonded water (q = 0.3, site I) and with 3 co-ordinated water molecules (q = 2.8, site II), respectively. The H_2L synthon is therefore an interesting building block for the design of elaborate compartmental ligands and/or of supramolecular functional assemblies.

Introduction

Many biomedical analyses rely on luminescence as a signal reporter since analytical methods based on this phenomenon are among the most sensitive available. Luminescent labels are being extensively developed for the design of efficient fluoro-immunoassays despite intrinsic limitations due to non-specific short-lived luminescence from the assay medium. This drawback is indeed easily overcome by the use of trivalent lanthanide ions Ln^{III} which have long-lived excited states (*e.g.* Eu^{III}, Tb^{III}).[1] Since f–f transitions are very weak, excitation of the metal ion is usually achieved by energy transfer from the bonded ligands, a process termed antenna effect[2] in reference to the naturally occurring phenomenon encountered in green plants.[3] The higher molar absorbance of the organic shell allows a better collection of the incident photons when compared to the free metal ions. This is especially true for lanthanide metal ions, for which the various selection rules make their electronic transitions strongly forbidden with molar absorption co-efficients rarely higher than a few $M^{-1}\,cm^{-1}$.[4]

Among the prerequisites for a good antenna system with potential as a label for time-resolved analysis or imaging of biological materials, criteria such as: high absorptivity of the compound, efficient energy transfer to the metal ion, shielding of the latter from vibrational deactivation processes, a long-lived metal-centred excited state, water solubility and thermodynamic and photophysical stability have to be fulfilled. Present-day technology in supramolecular chemistry allows a precise control of the metal co-ordination sphere and permits a fine-tuning of the energy-transfer processes either in simple devices used as luminescent stains[5] or in more elaborate molecular wires and sensors.[6] The choice of the ligand remains however a crucial point and molecules containing aromatic moieties are usually found to be good sensitisers for Ln^{III} ions[2,4,7] but more rarely meet all the above-mentioned criteria.[8]

In an effort to bring further understanding to the relationship between the ligand structure and the efficiency of the energy transfer process and, also, to unravel suitable synthons for the design of elaborate compartmental ligands, we have turned our attention to 2,2′-bipyridine-6,6′-dicarboxylic acid, H_2L.

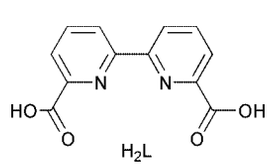

H_2L

Thanks to its aromatic core, combined with a four-site pincer-shaped co-ordinating pattern, H_2L appears as an interesting candidate for use as a light-harvesting moiety for lanthanide cations. Furthermore, the carboxylate functions are expected to provide suitable thermodynamic stability in water. The relative luminescence yield of 1 : 1 solutions of H_2L and Eu^{III} and Tb^{III} ions has been briefly reported by Mukkala *et al.*[9] within the framework of a study relating the influence of the chelating

† Electronic supplementary information (ESI) available: emission spectra for H_2L and $(Et_3NH)[TbL_2]$, excitation and emission spectra for $(Et_3NH)[EuL_2]$ and a stacking diagram for $[TbL_2\text{-}\mu\text{-}TbL(H_2O)_3]{\cdot}2H_2O{\cdot}2MeOH$. See http://www.rsc.org/suppdata/dt/b0/b000436g/

DOI: 10.1039/b000436g

groups on the luminescence properties of a series of lanthanide complexes, but no other data are available and the complexes were not isolated and characterised in the solid state. In this paper, we report the isolation and characterisation of two series of complexes with Ln = Eu, Gd, Tb and the deprotonated ligand together with the associated structural and photophysical data.

Results and discussion

Synthesis and characterisation of $(Et_3NH)[LnL_2]$ complexes (Ln = Eu, Gd, Tb)

The complexes were synthesised by reacting a twofold excess of the ligand with lanthanide nitrates in methanol and in the presence of triethylamine as a base, followed by re-crystallisation. In the case of europium, treatment with KPF_6 in hot water resulted in the replacement of the triethylammonium cation by potassium. IR spectra of the three metal complexes are very similar, showing the presence of absorption bands characteristic of the pyridine moiety ($\nu_{C=C}$ and $\nu_{C=N}$ around 1590 and 1570 cm^{-1}) and of the carboxylate groups ($\nu_{C=O}$ at 1637, 1640 and 1643 cm^{-1} respectively for Eu, Gd and Tb).[10] The absence of any absorption band that could be attributed to the nitrate group[11] unambiguously proves the displacement of the anion during the formation of the complexes. The ^{1}H-NMR spectrum of the europium complex in D_2O/d_6-DMSO displays three broad signals corresponding to the aromatic protons, with the expected coupling pattern (two doublets at 7.67 and 6.39 ppm and a triplet at 7.98 ppm, respectively 8.76, 8.15 and 8.21 for H_2L in d_6-DMSO), and pointing to the presence of two equivalent ligands on the NMR time scale. The presence of one triethylammonium cation is confirmed by the observation of a quadruplet and a triplet with integral values corresponding to 6 and 9 H respectively, as compared to the value of 4 protons for each aromatic signal. The de-shielding of the quadruplet at 2.99 ppm (2.43 ppm for neat Et_3N) confirms the protonation of the nitrogen atom.[12] The ^{1}H-NMR spectrum of the Tb chelate is stretched over 60 ppm at 298 K as a result of the paramagnetic contribution of the terbium ion.[13] The increase of the transverse relaxation rates for protons in the neighbourhood of the terbium cation leads to broad peaks and the hyperfine structure is lost. Nevertheless, the integral values of the peaks allows one to assign the aromatic protons at 17.88, −6.10 and −37.49 ppm and the ethyl protons of the ammonium cations at 3.38 and 1.44 ppm. The FAB^+/MS spectrum of $(Et_3NH)[TbL_2]\cdot 3H_2O$ shows an intense peak at $m/z = 645$ corresponding to the diprotonated complex $[Tb(LH)_2]^+$ as well as peaks at $m/z = 746$ and 847, attributed to the same species linked to respectively one and two triethylamine molecules. Measurements in the negative mode display a quasi single peak at m/z 643 attributed to $[TbL_2]^-$. Both NMR and MS data unambiguously point to the presence of a single species in solution, with a 1 : 2 metal : ligand stoichiometry.

The absorption spectrum of the protonated ligand H_2L, recorded in a 95/5 (v/v) water–DMSO mixture at room temperature shows a broad band at 297 nm ($\varepsilon = 6860\ M^{-1}\ cm^{-1}$) with a shoulder at 309 nm ($\varepsilon = 5800\ M^{-1}\ cm^{-1}$) attributed to $\pi\rightarrow\pi^*$ transitions on the pyridine rings (Fig. 1). Upon addition of triethylamine, the maximum of absorption is gradually shifted to higher energy, appearing at 288 nm ($\varepsilon = 8610\ M^{-1}\ cm^{-1}$) for a large excess of the base, while the position of the shoulder remains essentially unchanged ($\lambda_{max} = 310$ nm, $\varepsilon = 2600\ M^{-1}\ cm^{-1}$). Upon complexation to the lanthanide cations, the $\pi\rightarrow\pi^*$ transitions are shifted to lower energy, as often observed during the complexation of heteroaromatic systems with lanthanide cations.[14] The spectra of the three $(Et_3NH)[LnL_2]$ complexes (Ln = Eu, Gd and Tb) are very similar in their shape, with two maxima at 308 ($\varepsilon = 23\ 300\ M^{-1}\ cm^{-1}$) and 316 nm ($\varepsilon = 23\ 150\ M^{-1}\ cm^{-1}$) for Eu (Fig. 1), 306 ($\varepsilon = 18\ 800\ M^{-1}\ cm^{-1}$) and 315 nm ($\varepsilon = 20\ 100\ M^{-1}\ cm^{-1}$) for Gd and 308 ($\varepsilon = 24\ 300\ M^{-1}\ cm^{-1}$) and 318 nm ($\varepsilon = 24\ 750\ M^{-1}\ cm^{-1}$) for Tb. Due to the very low solubility of the complexes, the weak f–f absorption bands and, in the case of europium, the possible charge transfer band[15] could not be evidenced.

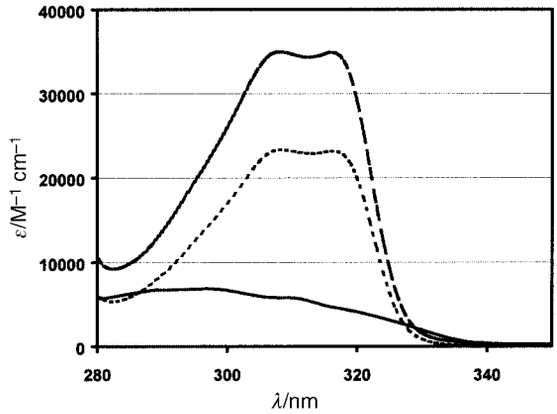

Fig. 1 UV-Vis spectra of solutions of H_2L (—), $(Et_3NH)[EuL_2]$ (– –) and $[Eu_2L_3(H_2O)_3]\cdot H_2O$ (— —) in DMSO/H_2O (5/95, v/v).

Ligand-centred luminescence in H_2L and $(Et_3NH)[GdL_2]$

In the solid state at 77 K, the protonated ligand presents two emission bands (Fig. S1, ESI)† upon excitation in the range 340–350 nm (maxima of the excitation spectra). One band centred at 390 nm is asymmetric with a tail in the long wavelength range and it disappears as soon as a time delay is enforced; we therefore assign it as arising from a $^1\pi\pi^*$ state. The other band is structured, with components at 492 nm (20 325 cm^{-1}, 0-phonon component), 525 nm (maximum), 558 and ≈600 nm. The main vibrational progression amounts to 1220 ± 80 cm^{-1} and corresponds to a ring breathing mode occurring at 1265 cm^{-1} in the fundamental state at room temperature, as inferred from the IR spectrum. The luminescence decay is bi-exponential, with lifetimes of 10.6 ± 0.1 and 2.3 ± 0.1 ms at 10 K. The long luminescence lifetimes and a ring breathing associated vibrational progression both point to a $^3\pi\pi^*$ state centred on the bipyridine rings. At room temperature, the emission spectrum remains essentially the same, except for the expected broadening and a slight red-shift. The luminescence quantum yield Q^L of a 10^{-6} M solution in water, is small and amounts to 0.76% at pH 9.9 ($\lambda_{exc} = 255$ nm) and 2.0% at pH 2.0 ($\lambda_{exc} = 227$ nm).

Upon complexation to Gd^{III}, the room temperature emission from the $^1\pi\pi^*$ state shifts to longer wavelength (391 nm) in the solid state, while the triplet state emission with lifetimes equal to 8.2 ± 0.2 and 4.3 ± 0.1 ms appears to be less affected. The quantum yield of the ligand-centred luminescence decreases to 0.36% for a 10^{-4} solution of $(Et_3NH)[GdL_2]$ in H_2O at pH 6.8 ($\lambda_{exc} = 282$ nm). No ligand-centred luminescence is observed for the Eu^{III} and Tb^{III} chelates, pointing to an efficient transfer of the excitation energy onto the metal ions.

Metal-centred luminescence in $(Et_3NH)[LnL_2]$ chelates (Ln = Eu, Tb)

The excitation spectrum of a solid sample of $(Et_3NH)[EuL_2]$ at 10 K (Fig. S2, ESI)† displays one broad and structured band with components at 331 nm, 342 nm (maximum), 350 and 357 nm, assigned to the $^1\pi\pi^*$ state of the ligand, as well as characteristic bands of the Eu^{III} ion, at 378.4 ($^5G_4\leftarrow{}^7F_0$), 382 ($^5G_2\leftarrow{}^7F_0$), 397 and 400 ($^5L_6\leftarrow{}^7F_0$), 466 ($^5D_2\leftarrow{}^7F_0$) and 528.5 nm ($^5D_1\leftarrow{}^7F_0$). The spectrum at 295 K is essentially identical with, in addition, excitation bands from the thermally populated $^7F_1$ level and a faint $^5D_0\leftarrow{}^7F_0$ transition (Fig. S2, ESI).† High resolution excitation and emission spectra of the $^5D_0\leftarrow{}^7F_0$ and $^5D_0\rightarrow{}^7F_0$ transitions (Fig. S3, ESI)† reveal one broad and

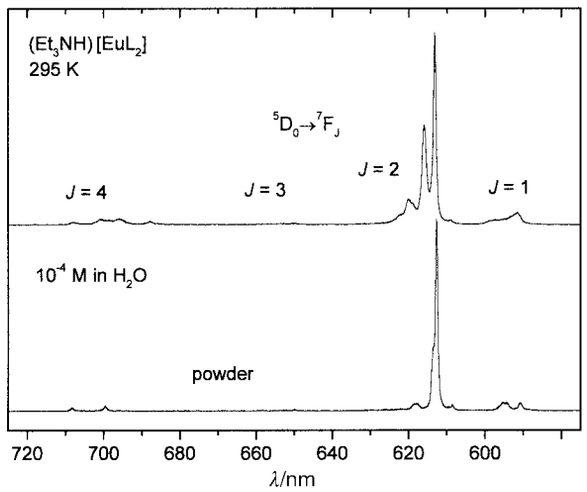

Fig. 2 Emission spectra of $(Et_3NH)[EuL_2]$ at 295 K in solution at pH = 6.6 (top, λ_{exc} = 395 nm) and in the solid state (bottom, λ_{exc} = 580.74 nm).

slightly asymmetric component centred at 581.13 nm at 10 K (site I) with a shoulder at 581.28 nm (site II) and 580.76 nm at 295 K. Selective laser excitation on the 0–0 transition at 10 K yields spectra typical of low symmetry species and dominated by the hypersensitive $^5D_0 \rightarrow {}^7F_2$ transition (Fig. S4, ESI).†

Relative corrected intensities of the $^5D_0 \rightarrow {}^7F_J$ transitions are 0.06, 1.00, 5.7, 0.1, and 0.32 for J = 0, 1, 2, 3, and 4, respectively. The spectra obtained by exciting site I and site II differ slightly in the splitting of the $^5D_0 \rightarrow {}^7F_1$ transition and in the relative intensity of the components of the $^5D_0 \rightarrow {}^7F_2$ transition. These differences disappear at room temperature and we assign them as arising from crystal defects rather than from two different metal-ion environments. Lifetime measurements have been performed exciting both the ligand $^1\pi\pi^*$ level and the $^5D_0$ level. Single exponential decays were observed in each case and the lifetime is constant both with respect to the excitation mode and to temperature between 10 and 295 K: 1.55 ± 0.08 ms. These observations point to an Eu environment free of inner sphere water molecules and fairly rigid.

The relative intensities of the $^5D_0 \rightarrow {}^7F_J$ transitions of a 10^{-4} M solution of the chelate in degassed water (pH 6.6, 295 K) are similar to those found for the solid state sample (0.004, 1.00, 6.81, 0.11 and 0.65 for J = 0, 1, 2, 3 and 4 respectively), but the crystal field splitting is much altered, pointing to strong interaction with water (Fig. 2). As a result, the Eu($^5D_0$) decay time is shortened to 0.86 ± 0.02 ms, corresponding to k_{H_2O} = 1.16 ms^{-1}, but remains monoexponential. Taking into account the commonly encountered value of 0.5 ms^{-1} for the radiative rate constant k_{D_2O},[16] or the one deduced from the solid state lifetime, and using the newly proposed equation allowing for the presence of closely diffusing water molecules, $q = 1.2\ (k_{H_2O} - k_{D_2O} - 0.15)$,[16] this decay time reflects the quenching effect of 0.4–0.6 water molecules directly bonded to the Eu(III) ion.[4] This may be interpreted as reflecting some inner sphere interaction with fast exchanging water molecules. The absolute quantum yield of the metal-centred luminescence of this solution is fairly large, amounting to 11.5 ± 2.3% and in line with the 0-phonon component of the ligand triplet state lying about 3000 cm^{-1} above the Eu($^5D_0$) level.[17] In their work on water solutions with a 1:1 $Eu^{III}:H_2L$ ratio, Mukkala *et al.* have found a bi-exponential decay with lifetimes of 0.77 and 0.19 ms at pH 8.5 and they assigned the two lifetimes to complexes with different metal-to-ligand ratios.[9] Using the same procedure as above to estimate q, the lifetimes reported by Mukkala's group at this pH correspond to approximately 0.8 and 5.5 inner sphere water molecules, respectively. Given the difference in the experimental conditions, our data are in good agreement with those reported by Mukkala *et al.* for the 1:2 complex.[9]

At 77 K and upon excitation at both 330 ($^1\pi\pi^*$) and 488 nm ($^5D_4$) a solid state sample of the Tb^{III} chelate displays an emission spectrum dominated by the $^5D_4 \rightarrow {}^7F_5$ transition (Fig. S5, ESI)† which fades out at room temperature. In parallel, the Tb($^5D_4$) lifetime decreases sharply from 1.24 ± 0.01 ms at 77 K to 0.21 ± 0.01 ms at 295 K, pointing to a temperature activated energy back transfer process from the Tb($^5D_4$) level to the ligand levels.[15,18] This behaviour is understandable since the energy of the 0-phonon component of the $^3\pi\pi^*$ ligand state at 20 325 cm^{-1} is in resonance with the $^5D_4$ state, the sub-levels of which extend from 20 050 to 20 480 cm^{-1}. As a consequence, the absolute quantum yield of the metal-centred luminescence displayed by a 10^{-4} M solution at pH = 6.6 is lower than the one found for the Eu^{III} chelate, amounting to 6.3 ± 1.3%.

Synthesis and characterisation of $[Ln_2L_3(H_2O)_3]\cdot xH_2O$ complexes (x = 1, Ln = Eu, Tb; x = 0, Ln = Gd)

The complexes were crystallised from equimolar solutions of the ligand and the lanthanide nitrate in a methanol/water mixture, in the presence of triethylamine. Surprisingly, elemental analyses point to the formation of compounds with a 2:3 metal-to-ligand ratio and containing respectively four, three and four water molecules for Eu, Gd and Tb. The IR of the three complexes are quite similar and display features characteristic of the bipyridine ligands ($\nu_{C=N}$, $\nu_{C=C}$ and $\nu_{C=O}$ at 1617, 1615 and 1620 cm^{-1} respectively for Eu, Gd and Tb) but do not contain bands from nitrate anions. Interestingly, the $\nu_{C=O}$ absorption bands are observed at weaker energy than in the corresponding ML_2 complexes with a difference of about 20 cm^{-1}. This difference points to a somewhat weakened C=O bond, the electronic density of the carboxylate functions being displaced toward the metal binding oxygen atoms.

When dissolved in d_6-DMSO or D_2O the solutions of the europium or terbium complexes show a mixture of 1:1 and 1:2 chelates, as demonstrated by the ^{1}H-NMR for which two sets of signals in a 1:2 ratio are observed. For Eu, the signals arising from the first set, assigned to an ML_2^- entity is composed of a triplet (10.20 ppm) and two doublets (13.32 and 7.07 ppm) with coupling constants ^3J = 7.8 Hz; the second set, attributed to an ML^+ entity, is also comprised of a triplet at 4.34 ppm, and two doublets at 4.52 and −2.36 ppm, with the same coupling constant (7.8 Hz). As previously mentioned, the paramagnetic contribution of Tb^{III} leads to a spectrum spread over 160 ppm. Signals from the 1:2 species appear at 17.97, −22.20 and −76.67 ppm while signals from the 1:1 chelate appear at 75.28, 20.74 and −4.62 ppm. The comparison of the chemical shifts of the $[LnL_2]^-$ complexes (*vide supra*) with those of the equivalent sets for the $[M_2L_3(H_2O)_3]$ solutions, shows the two entities to be significantly different in solution. The presence of a second paramagnetic metal atom in the latter case increases the magnetic susceptibility of the bulk.[19] If this point alone is taken into account and if one assumes that both metallic entities are weakly coupled, a constant difference $\Delta\delta$ between the chemical shifts for a proton in each type of complex is expected,[19] which has not been observed in our case. Furthermore, we note that the pattern distribution in $[EuL_2]^-$ (triplet, doublet and doublet from low to high fields) is different from that in $[Eu_2L_3(H_2O)_3]$ (doublet, triplet and doublet). Two possible explanations can be formulated: (i) an important magnetic coupling takes place between the metal ions or (ii) a close contact pairing is retained in solution between the $[ML_2]^-$ and $[ML]^+$ moieties. In view of the known weak magnetic interaction taking place between two f-metal ions separated by a distance larger than 4 Å and of the solid state structure of $[Tb_2L_3(H_2O)_3]\cdot H_2O$ described below, the second explanation is favoured. Whatever the metal ion, Eu^{III} or Tb^{III}, the two sets of signals clearly indicate that no ligand exchange occurs at room temperature on the NMR time scale, pointing to species stable in water, with no interconversion between them, an important prerequisite for biomedical appli-

Table 1 Selected bond lengths (Å) and angles (°) in $[TbL_2\text{-}\mu\text{-}TbL(H_2O)_3]\cdot 2H_2O\cdot 2MeOH$

Tb1–O1	2.334(2)	Tb2–O8	2.329(2)
Tb1–N1	2.518(3)	Tb2–O9	2.355(3)
Tb1–N2	2.494(3)	Tb2–N5	2.524(3)
Tb1–O3	2.324(3)	Tb2–N6	2.511(3)
Tb1–O5	2.324(2)	Tb2–O11	2.306(2)
Tb1–N3	2.503(3)	Tb2–O13	2.372(2)
Tb1–N4	2.511(3)	Tb2–O14	2.410(3)
Tb1–O7	2.377(2)	Tb2–O15	2.425(2)

Atom(*x*)–Tb1–Atom(*y*)

	O1	N1	N2	O3	O5	N3	N4
N1	65.87(9)						
N2	128.72(9)	62.97(9)					
O3	165.08(9)	129.03(9)	66.11(9)				
O5	97.84(9)	80.05(9)	76.97(8)	86.8(1)			
N3	85.25(9)	131.59(9)	133.08(9)	83.76(9)	65.79(8)		
N4	81.29(9)	139.91(9)	141.01(8)	84.74(9)	128.76(8)	63.08(9)	
O7	91.82(9)	92.00(8)	86.66(8)	87.17(9)	163.62(8)	128.55(8)	65.70(8)

Atom(*x*)–Tb2–Atom(*y*)

	O8	O9	N5	N6	O11	O13	O14
O9	92.93(9)						
N5	82.95(9)	65.04(9)					
N6	76.11(8)	127.66(9)	62.89(9)				
O11	86.76(9)	165.69(9)	128.97(8)	66.12(8)			
O13	146.52(8)	99.76(9)	74.79(9)	71.59(8)	88.13(9)		
O14	145.11(9)	79.8(1)	122.7(1)	134.60(8)	92.3(1)	68.14(8)	
O15	76.19(9)	84.6(1)	142.10(9)	138.02(9)	81.42(9)	135.49(9)	69.19(9)

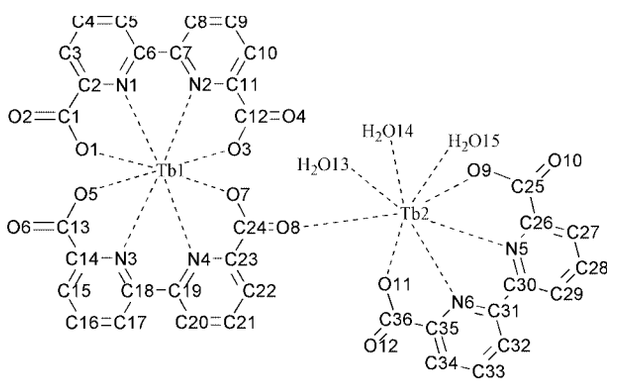

Fig. 3 The atom numbering scheme for $[TbL_2\text{-}\mu\text{-}TbL(H_2O)_3]\cdot 2H_2O\cdot 2MeOH$.

cations. The FAB^+/MS spectrum of $[Tb_2L_3(H_2O)_3]$ indicates the presence of a $[Tb(LH)_2]^+$ species ($m/z = 645$) and $\{[Tb_2L_3\cdot 3H_2O] + 2H\}^{2+}$ entities ($m/z = 551$).

Absorption spectra of solutions of the three complexes are very similar. The $\pi\rightarrow\pi^*$ transitions on the bipyridine moieties are shifted to lower energy with respect to the free ligand. The absorption bands display two maxima in each case at 308 ($\varepsilon = 34\,950\ M^{-1}\ cm^{-1}$) and 316 nm (34 900) for Eu, 307 (37 750) and 318 nm (36 800) for Gd and 307 (37 100) and 316 nm (37 300) for Tb. The shapes of these spectra closely resemble those of the spectra generated by the $(Et_3NH)[LnL_2]$ chelates but the molar absorption coefficients are nearly 1.5 times larger, as expected on the basis of the number of ligands per lanthanide cation (Fig. 1).

X-Ray crystal structure of $[Tb_2L_3(H_2O)_3]\cdot 2H_2O\cdot 2MeOH$

Selected bond lengths and angles are listed in Table 1 while the atom-numbering is shown on Fig. 3. The structure is comprised of discrete and neutral supramolecular dimeric units (Fig. 4). One of the metal ions is 8-coordinate, being bonded to the four N atoms of two ligand molecules (mean bond length 2.50(1) Å) and to the four carboxylate groups (mean bond length 2.34(3) Å). The two ligand molecules are almost planar and lie perpendicular to each other. The second 8-co-ordinate Tb^{III} ion is bonded to one de-protonated ligand molecule (mean Tb2–N: 2.51(1) Å, mean Tb2–O 2.33(2) Å) and completes its co-ordination sphere by binding three water molecules (mean Tb2–O 2.40(3) Å) and one O atom from a bridging carboxylate group attached to a ligand molecule bonded to Tb1 (mean Tb2–O = 2.33 Å). As a consequence, the Tb1–O(carboxylate) distance is substantially longer (mean 2.38 Å) than the three other ones (mean 2.33(1) Å). The correct formulation of the 2:3 complex is therefore $[TbL_2\text{-}\mu\text{-}TbL(H_2O)_3]\cdot 2H_2O\cdot 2MeOH$ and the intermolecular Tb1–Tb2 distance amounts to 6.51 Å.

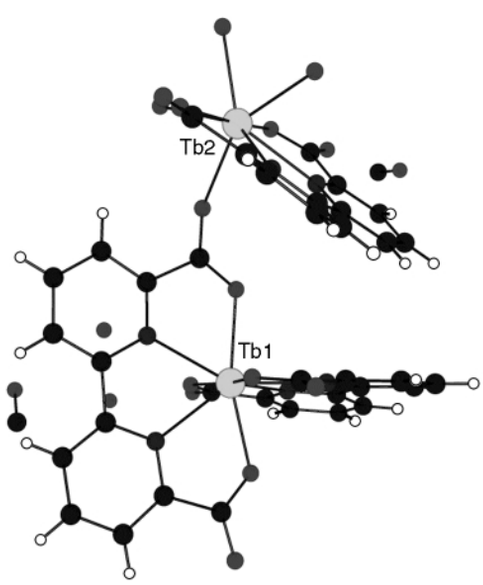

Fig. 4 View of the dimeric unit in $[TbL_2\text{-}\mu\text{-}TbL(H_2O)_3]\cdot 2H_2O\cdot 2MeOH$.

Two consecutive dimers are connected by an elaborate network of hydrogen bonds involving the solvation molecules (Fig. 5). One methanol molecule (O18) is connected through H-bonding to a carboxylic O-atom of the ligand bound to Tb2 (O18 · · · O12 = 2.68 Å) while the other methanol molecule (O19) is H-bonded to both a co-ordinated water molecule (O19 · · · O14 = 2.70 Å) and, more weakly, to the interstitial O17 water molecule (O19 · · · O17 = 2.96 Å), itself H-bonded to one carboxylate linked to Tb1 (O17 · · · O1 = 2.85 Å). The second

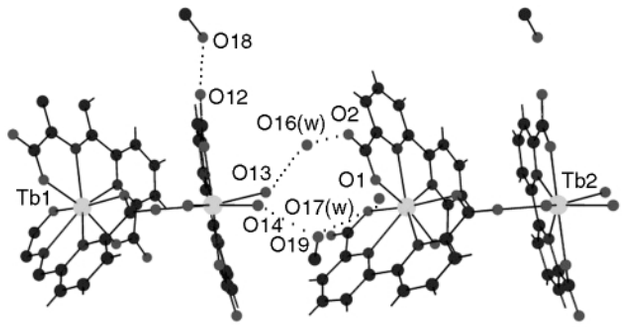

Fig. 5 H-bonds network connecting two dimeric units in $[TbL_2\text{-}\mu\text{-}TbL(H_2O)_3]\cdot 2H_2O\cdot 2MeOH$.

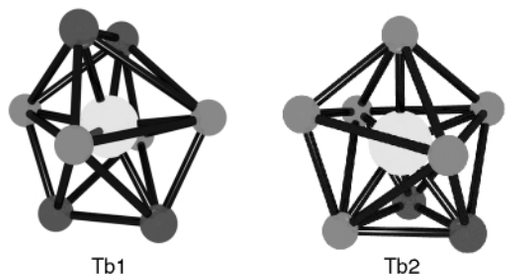

Fig. 6 Co-ordination polyhedra in $[TbL_2\text{-}\mu\text{-}TbL(H_2O)_3]\cdot 2H_2O\cdot 2MeOH$.

interstitial water molecule bridges two dimeric entities, being H-bonded to a carboxylate co-ordinated to Tb1 (O16 · · · O2 = 2.71 Å) and to a water molecule bound to Tb2 (O16 · · · O13 = 2.66 Å). The dimers are aligned in the crystal, forming parallel cylinders with no interaction between them (Fig. S6, ESI).† Within a stack the Tb1–Tb1 and Tb2–Tb2 distances between metal ions belonging to two consecutive dimers are equal and amount to 13.7 Å, while the metal–metal distance between columnar stacks of molecules is much larger (around 24–25 Å). The co-ordination polyhedron around Tb1 may be described as a distorted C_{2v} dodecahedron (Fig. 6), the four O-atoms forming an approximate square plane while the N-atoms of each ligand sit above and below this plane, respectively, and are aligned along the two diagonals of the square. The co-ordination geometry around Tb2 displays lower symmetry and can be classified as a 1 : 4 : 3 polyhedron.

Photophysical properties of $[Eu_2L_3(H_2O)_3]\cdot H_2O$

At room temperature, the $^5D_0\leftarrow{}^7F_0$ excitation spectrum of the solid state Eu compound reveals two broad bands at 580.05 nm (site I) and 579.76 nm (site II). Selective laser excitation of these two components yields two different spectra dominated by the $^5D_0\rightarrow{}^7F_2$ transition and typical of Eu^{III} in low-symmetry co-ordination sites (Fig. 7). The Eu^{III} ions in site I experience a larger crystal field effect than in site II, *e.g.* a total separation of 153 cm^{-1} *vs.* 103 cm^{-1} for the $^7F_1$ sub-levels and of 192 cm^{-1} *vs.* 141 cm^{-1} for the $^7F_2$ sub-level (Table 2). Moreover, the Eu($^5D_0$) lifetime is longer in site I (1.23 ± 0.02 ms) than in site II (0.32 ± 0.01 ms) and taking into account the same radiative rate constant as above, the following number of bonded water molecules can be calculated: $q = 0.3$ for site I and 2.8 for site II. The former value is small and may be accounted for by the presence of closely diffusing OH oscillators in the second co-ordination sphere of the metal ion.[16] Therefore, the luminescence data point to a structure similar to the one evidenced by X-ray crystallography for the Tb^{III} bimetallic chelate, site I corresponding to Tb1 and site II to Tb2. In addition, the energy of the measured $^5D_0\leftarrow{}^7F_0$ transitions for the two sites is in keeping with this explanation. Frey and Horrocks have demonstrated that a correlation exists between the energy of the 0–0 transition, that is the position of the $^5D_0$ level, and parameters

Table 2 Identified Eu(^7F_J) crystal field sub-levels (cm^{-1}, origin $^7F_0$, $J = 1$–4) in solid samples of $(Et_3NH)[EuL_2]$ and $[Eu_2L_3(H_2O)_3]$, as determined from emission spectra at 295 K

		$[Eu_2L_3(H_2O)_3]$	
Level	$(Et_3NH)[EuL_2]$	Site I	Site II
$^7F_1$	290	273	274
	395	375	303
	416	426	377
$^7F_2$	784	921	927
	898	943	957
	920	996	1006
	1029	1029	1035
	1048	1113	1068
$^7F_3$	1832	1864	1856
	1893		1875
			1939
$^7F_4$	2848	2752	2704
	2925	2825	2840
	3101	2951	2870
		3002	2967
		3085	3032
			3096

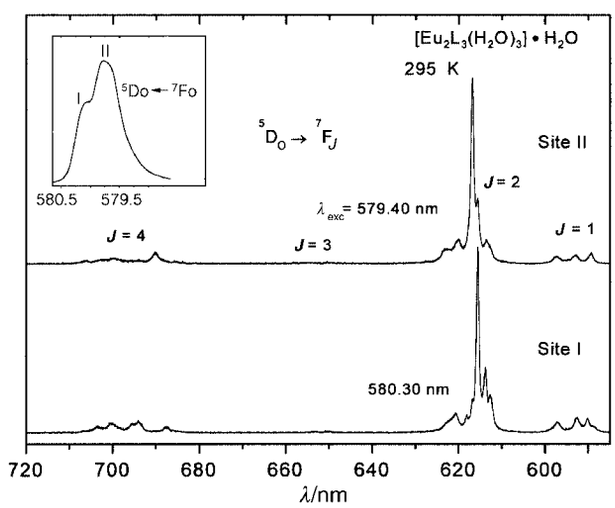

Fig. 7 Emission spectra of $[Eu_2L_3(H_2O)_3]\cdot H_2O$ under selective excitation at 295 K displaying the two different co-ordination environments for Eu^{III}. Inset: excitation spectrum of the 0–0 transition.

describing the ability δ of co-ordinating atoms to produce a nephelauxetic effect:[20]

$$\tilde{\nu} - \tilde{\nu}_0 = C_{CN} \sum_i n_i \delta_i$$

where C_{CN} is a coefficient depending upon the Eu^{III} co-ordination number (1.06 for a co-ordination number (CN) = 8), n_i is the number of atoms of type i, and $\tilde{\nu}_0 = 17\,374$ cm^{-1} at 295 K.[20] Using $\delta_{OOC} = -17.2$,[20] $\delta_{H_2O} = -10.2$,[20] and the nephelauxetic parameter deduced from previous studies on heterocyclic imines, $\delta_{N=C} = -15.3$,[8] we predict $\tilde{\nu}$ (site I) = 17 236 cm^{-1} and $\tilde{\nu}$ (site II) = 17 254 cm^{-1}, in agreement with the measured values of 17 240 and 17 248.5 cm^{-1}, respectively.

Upon lowering the temperature, the general features described above are retained, but the situation becomes more complicated, with new components appearing on the $^5D_0\leftarrow{}^7F_0$ excitation spectrum, probably arising from rearrangement in the H-bond network. Further analysis was therefore not carried out. Moreover, the back transfer process occurring for the Tb^{III} bimetallic chelate also prevented a detailed analysis of the Tb($^5D_4$) lifetimes.

Conclusion

The ligand 2,2′-bipyridine-6,6′-dicarboxylic acid in its dianionic form appears to be a good building block for designing

extended ligands aimed at complexing and sensitising trivalent luminescent europium and terbium ions. It efficiently binds the cations in a planar tetradentate co-ordinating mode, leading to two series of complexes in which the ligand to lanthanide stoichiometry is different. In the first series labelled $(Et_3NH)[LnL_2]$ a single lanthanide species $[LnL_2]^-$ is present in solution, while in the second series labelled $[LnL_3\cdot(H_2O)_3]$ two lanthanide entities $[LnL]^+$ and $[LnL_2]^-$ are observed in solution, with some peculiar interactions deduced from ^{1}H-NMR. In the solid state, these latter moieties formed a neutral bimetallic entity which was characterised for Tb by an X-ray structure determination and luminescence spectroscopy. The bipyridine moieties are confirmed as providing a good antenna effect[21] and the formation of an extended network of H-bonded bimetallic entities in the 2:3 compounds opens the way for tailoring compartmental ligands bearing H_2L units or bipyridine monocarboxylic acids and programmed for the formation of extended interactions at a nanometric scale.

Experimental

Syntheses and characterisation

Solvents and starting materials were purchased from Fluka, lanthanide nitrates (99.9%) from Janssen Chimica. 2,2′-Bipyridine-6,6′-dicarboxylic acid was prepared in 87% yield by oxidation of 6,6′-dimethyl-2,2′-bipyridine[22] with CrO_3 in concentrated sulfuric acid, using an adapted literature procedure.[23] IR spectra were recorded as KBr pellets on a Nicolet 210 spectrometer. UV-Vis spectra of solutions in 95/5 (v/v) H_2O/DMSO were obtained with a Uvikon 933 spectrophotometer. ^{1}H-NMR spectra were recorded at 298 K with a Bruker AC 200 spectrometer using the peak of the solvent as internal reference or *tert*-BuOH for spectra in D_2O. Luminescence spectra were measured according to previously published procedures.[24] Absolute quantum yields of the ligand-centred luminescence were determined with respect to quinine sulfate 2×10^{-7} M in H_2SO_4 0.05 M (absolute quantum yield 0.546),[25] while those of the metal-centred luminescence were measured using $[Ln(tpy)_3](ClO_4)_3$ 10^{-3} M as standards (absolute quantum yields: 1.3 (Eu) and 4.7% (Tb)).[24]

$(Et_3NH)[LnL_2]$, general procedure

To a suspension of H_2L (2×10^{-4} mol) in 10 cm^3 MeOH, were added 3 cm^3 of a solution of $Ln(NO_3)\cdot xH_2O$ (10^{-4} mol, $x = 6$, 5 and 6 for Eu, Gd and Tb, respectively) in MeOH. After 15 min stirring, the solution was evaporated to dryness, suspended in 30 cm^3 water and 0.15 cm^3 neat triethylamine was added. The mixture was heated to reflux until all the solid was dissolved, filtered and concentrated to 2 cm^3. Upon concentration, a solid formed and 20 cm^3 of THF were added before cooling the solution to 4 °C. The solid was separated by centrifugation and dried under vacuum.

$(Et_3NH)[TbL_2]\cdot 3H_2O$. Yield 80%. [Found: C, 44.79; H, 4.02; N, 8.61. $C_{30}H_{28}TbN_5O_8\cdot 3H_2O$ requires C, 45.10; H, 4.29; N, 8.76%]. δ_H (D_2O/*tert*-BuOH) 17.88 (s, 8 H, br), 3.38 (s, 6 H, br), 1.44 (s, 9 H, br), −6.10 (s, 8 H, br), −37.49 (s, 8 H, br). ν_{CO} 1643 cm^{-1}, $\nu_{C=C}$ and $\nu_{C=N}$ 1597 and 1571 cm^{-1}, ν_{CH} (aromatic) 780 cm^{-1}. FAB+/MS: 645 ($[Tb(LH)_2]^+$), 746 ($[Tb(LH)L\cdot Et_3NH]^+$), 847 ($[TbL_2\cdot(Et_3NH)_2]^+$). FAB−/MS: 643 ($[Tb(L)_2]^-$).

$(Et_3NH)[EuL_2]$. Obtained as described previously (yield 86%. δ_H (D_2O/d_6-DMSO, 50/50 v/v) 7.98 (t, br, 4 H, $^3J = 8.0$ Hz), 7.67 (d, br, 4 H, $^3J = 7.7$ Hz), 6.39 (d, br, 4H, $^3J = 6.6$ Hz), 2.99 (q, 6H, $^3J = 7.2$ Hz), 1.12 (t, 9H, $^3J = 7.0$ Hz). IR (cm^{-1}) ν_{CO} 1637, $\nu_{C=C}$ and $\nu_{C=N}$ 1592 and 1571, ν_{CH} (aromatic) 776).

$K[EuL_2]\cdot 3H_2O$. Two equivalents of KPF_6 were added to a warm water solution of $(Et_3NH)[EuL_2]$ and the solution was slowly concentrated and cooled to 4 °C. The solid was recovered by centrifugation and was dried under vacuum. [Found: C, 39.42; H, 2.30; N, 7.41. $C_{24}H_{12}EuN_4O_8K\cdot 3H_2O$ requires C, 39.50; H, 2.49; N, 7.68%]. ν_{CO} 1655 cm^{-1}, $\nu_{C=C}$ and $\nu_{C=N}$ 1597 and 1571 cm^{-1}, ν_{CH} (aromatic) 778 cm^{-1}.

$(Et_3NH)[GdL_2]\cdot 2H_2O$. Yield 72%. IR (cm^{-1}) ν_{CO} 1640, $\nu_{C=C}$ and $\nu_{C=N}$ 1597 and 1570, ν_{CH} (aromatic) 778 cm^{-1}. (Found: C, 46.09; H, 3.98; N, 8.75. $C_{30}H_{28}GdN_5O_8\cdot 2H_2O$ requires C, 46.20; H, 4.14; N, 8.98%).

$[Ln_2L_3(H_2O)_3]\cdot xH_2O$, general procedure

A quantity of 2×10^{-4} mol of $Ln(NO_3)\cdot xH_2O$ ($x = 6$, 5 and 6 for Eu, Gd and Tb, respectively) was added to a suspension of H_2L (2×10^{-4} mol) in 20 cm^3 MeOH. Then 0.100 cm^3 of triethylamine in 10 cm^3 water was added and the solution was stirred for 15 min and filtered. The methanol was evaporated under reduced pressure and the solution was concentrated to 2 cm^3 and cooled to 4 °C. A precipitate formed, which was collected by centrifugation, washed with cold methanol and dried under vacuum.

$[Eu_2L_3(H_2O)_3]\cdot H_2O$. Yield 63%. [Found: C, 39.22; H, 2.38; N, 7.62. $C_{36}H_{24}Eu_2N_6O_{15}\cdot H_2O$ requires C, 39.45; H, 2.53; N, 7.53%]. δ_H (d_6-DMSO) 13.32 (d, 4 H, $^3J = 7.8$ Hz), 10.20 (t, 4 H, $^3J = 7.8$ Hz), 7.07 (d, 4 H, $^3J = 7.4$ Hz), 4.52 (d, 2 H, $^3J = 7.8$ Hz), 4.34 (t, 2H, $^3J = 7.8$ Hz), −2.36 (d, 2 H, $^3J = 7.8$ Hz). ν_{OH} 3420 cm^{-1}, ν_{CO} 1617 cm^{-1}, $\nu_{C=C}$ and $\nu_{C=N}$ 1592 and 1571 cm^{-1}, ν_{CH} (aromatic) 775 cm^{-1}.

$[Tb_2L_3(H_2O)_3]\cdot H_2O$. Yield 56%. [Found: C, 39.07; H, 2.61; N, 7.49. $C_{36}H_{24}N_6O_{15}Tb_2\cdot H_2O$ requires C, 38.73; H, 2.35; N, 7.53%]. δ_H (d_6-DMSO) 75.28 (s, 2 H, br), 20.74 (s, 2 H, br), 17.97 (s, 4 H, br), −4.62 (s, 2 H, br), −22.20 (s, 4 H, br), −76.67 (s, 4 H, br). ν_{OH} 3415 cm^{-1}, ν_{CO} 1620 cm^{-1}, $\nu_{C=C}$ and $\nu_{C=N}$ 1597 and 1572 cm^{-1}, ν_{CH} (aromatic) 773 cm^{-1}.

$[Gd_2L_3(H_2O)_3]$. Yield 70%. [Found: C, 39.80; H, 2.48; N, 7.67. $C_{36}H_{24}Gd_2N_6O_{15}$ requires C, 39.48; H, 2.21; N, 7.67%]. ν_{OH} 3405 cm^{-1}, ν_{CO} 1615, $\nu_{C=C}$ and $\nu_{C=N}$ 1587 and 1560 cm^{-1}, ν_{CH} (aromatic) 772 cm^{-1}.

Crystal structure determination of $[Tb_2L_3\cdot 3H_2O]\cdot 2H_2O\cdot 2MeOH$

Single crystals of $[TbL_2\text{-}\mu\text{-}TbL(H_2O)_3]\cdot 2H_2O\cdot 2MeOH$ were obtained as thin colourless needles from dissolution of the title compound in hot water followed by slow cooling. A crystal was mounted in inert oil and transferred to the cold gas stream of the diffractometer. Crystal data and structure refinement details are listed in Table 3.

CCDC reference number 186/1936.

See http://www.rsc.org/suppdata/dt/b0/b000436g/ for crystallographic files in .cif format.

Table 3 Crystal data and structure refinement for $[TbL_2\text{-}\mu\text{-}TbL(H_2O)_3]\cdot 2H_2O\cdot 2MeOH$

Formula	$C_{36}H_{24}N_6O_{15}Tb_2\cdot 2H_2O\cdot 2CH_3OH$
Molecular weight	1198.59
Crystal system	Monoclinic
Space group	$P1\ 2_1/c\ 1$
a/Å	13.6780(5)
b/Å	18.930(1)
c/Å	15.8188(9)
β/°	92.227(3)
V/Å^3	4092.8(6)
Z	4
μ/mm^{-1}	3.518
T/K	173
Number of data measured	25474
Number of data with $I > 3\sigma(I)$	15332
R	0.037
R_w	0.053

Acknowledgements

We gratefully acknowledge Ms Véronique Foiret for her technical assistance in luminescence measurements. We thank the Fondation Herbette (Lausanne) for a gift of spectroscopic equipment. This work is supported through grants from the French Centre National de la Recherche Scientifique and the Swiss National Science Foundation. Professsor Jean Fischer, Dr André De Cian and Nathalie Kyritsakas from the Laboratoire de Cristallochimie et de Chimie Structurale from Strasbourg are acknowledged for the X-ray structure determination.

References

1 I. Hemmilä, T. Ståhlberg and P. Mottram, *Bioanalytical applications of labelling technologies*, 2nd edition, Wallac Oy, Turkey, 1995.
2 N. Sabbatini, M. Guardigli and J.-M. Lehn, *Coord. Chem. Rev.*, 1993, **123**, 201.
3 H. T. Witts, *New J. Chem.*, 1987, **11**, 91.
4 J.-C. G. Bünzli, in *Lanthanide Probes in Life*, *Chemical and Earth Science: Theory and Practice*, J.-C. G. Bünzli and G. R. Choppin, eds., Elsevier Scientific Publishers, B.V., Amsterdam, 1989.
5 C. Piguet and J.-C. G. Bünzli, *Chem. Soc. Rev.*, 1999, **28**, 347.
6 R. F. Ziessel, *J. Chem. Educ.*, 1997, **74**, 673.
7 V. Balzani and F. Scandola, *Supramolecular Photochemistry*, 1991, Ellis Horwood Ltd, Chichester, England.
8 M. Elhabiri, R. Scopelliti, J.-C. G. Bünzli and C. Piguet, *J. Am. Chem. Soc.*, 1999, **121**, 10747.
9 V.-M. Mukkala, M. Kwiatkowski, J. Kankare and H. Takalo, *Helv. Chim. Acta*, 1993, **76**, 893.
10 R. M. Silverstein and G. C. Bassler, *Identification spectrométrique des composés organiques*, Gauthier-Villars, Paris, 1968.
11 K. Nakamoto, *Infrared and Raman Spectra of Inorganic and Coordination Compounds*, 4th edition, Wiley, New York, 1986, p. 254.
12 C. D. Gutsche, M. Iqbal and I. Alam, *J. Am. Chem. Soc.*, 1987, **109**, 4314.
13 I. Bertini and C. Luchinat, *NMR of Paramagnetic Molecules in Biological Systems*, Benjamin/Cummings Publishing Co., Inc., Menlo Park, CA, 1986.
14 C. Piguet, J.-C. G. Bünzli, G. Bernardinelli, G. Hopfgartner and A. F. Williams, *J. Am. Chem. Soc.*, 1993, **115**, 8197.
15 L. J. Charbonnière, C. Balsiger, K. J. Schenk and J.-C. G. Bünzli, *J. Chem. Soc.*, *Dalton Trans.*, 1998, 505.
16 A. Beeby, I. M. Clarkson, R. S. Dickins, S. Faulkner, D. Parker, L. Royle, A. S. de Sousa, J. A. G. Williams and M. Woods, *J. Chem. Soc.*, *Perkin Trans. 2*, 1999, 493.
17 M. Latva, H. Takalo, V.-M. Mukkala, C. Matachescu, J.-C. Rodriguez-Ubis and J. Kankare, *J. Lumin.*, 1997, **75**, 149.
18 M. Kleinerman and C. Sang-Il, *J. Chem. Phys.*, 1968, **49**, 3901.
19 C. Piguet, E. Rivara-Minten, G. Hopfgartner and J.-C. G. Bünzli, *Helv. Chim. Acta*, 1995, **78**, 1651; L. J. Charbonnière, A. F. Williams, C. Piguet, G. Bernardinelli and E. Rivara-Minten, *Chem. Eur. J.*, 1998, **4**, 485.
20 S. T. Frey and W. deW. Horrocks Jr., *Inorg. Chim. Acta*, 1995, **229**, 383.
21 B. Alpha, J.-M. Lehn and G. Mathis, *Angew. Chem.*, *Int. Ed. Engl.*, 1987, **26**, 266.
22 T. Rode and E. Breitmaier, *Synthesis*, 1987, 574.
23 G. H. Cooper and R. L. Richard, *Synthesis*, 1971, 31.
24 S. Petoud, J.-C. G. Bünzli, K. J. Schenk and C. Piguet, *Inorg. Chem.*, 1997, **36**, 1345.
25 S. R. Meech and D. C. Phillips, *J. Photochem.*, 1983, **23**, 193.